

Beyond Imprecise Distance Metrics: Trace-Guided Directed Greybox Fuzzing via LLM-Predicted Call Stacks

YIFAN ZHANG, Peking University, China

XIN ZHANG*, Peking University, China

Directed greybox fuzzing (DGF) aims to efficiently trigger bugs at specific target locations by prioritizing seeds whose execution paths are more likely to reach the targets. However, existing DGF approaches suffer from imprecise potential estimation due to their reliance on static-analysis-based distance metrics. The over-approximation inherent in static analysis causes many seeds with execution paths irrelevant to vulnerability triggering to be mistakenly prioritized, significantly reducing fuzzing efficiency. To address this issue, we propose trace-guided directed greybox fuzzing (TDGF). TDGF replaces static-analysis-based distance metrics with vulnerability-oriented execution information (referred to as guidance traces) to steer directed fuzzing: seeds whose execution paths overlap more with the guidance traces are scheduled earlier for mutation. We empirically study two representative types of guidance traces: the control-flow trace and the call-stack trace of vulnerability-triggering executions. We find that the fine-grained control-flow traces offer nearly the same guidance capability as the coarse-grained call-stack traces, while call-stack traces are also easier for large language models (LLMs) to predict. Based on this insight, we further propose a framework that leverages LLMs to predict the call stack at vulnerability-triggering time and uses it to guide DGF. We implement our approach and evaluate it against several state-of-the-art fuzzers with experiments totaling 58.4 CPU-years. On a suite of real-world programs, our approach triggers vulnerabilities 2.13× to 3.14× faster than the baselines. Moreover, through directed patch testing on the latest program versions used in our controlled experiments, our approach discovers 10 new vulnerabilities and 2 incomplete fixes, with 10 assigned CVE IDs.

1 Introduction

Directed greybox fuzzing (DGF) [5] is currently one of the most effective tools for triggering bugs at specific locations. For each seed, DGF collects its execution path and uses specific strategies to calculate the potential of triggering target vulnerabilities through mutation, prioritizing the mutation of seeds with higher potential. As a result, DGF can trigger target vulnerabilities more quickly compared to conventional coverage-guided greybox fuzzing (CGF) [42]. Research related to DGF [5, 7, 11, 16, 19, 21, 22, 25] has been widely proposed and is also extensively applied in areas such as vulnerability reproduction, patch testing, and validation of static analysis alarms.

However, existing DGF approaches are still imprecise in calculating mutation potential toward the target. Existing DGF approaches calculate potential based on complex distance metrics, such as distances on the control flow graph (CFG) and value flow graph (VFG). The computation of these distances is derived from over-approximations in static analysis, which inevitably leads to **many flows that do not exist during actual execution that triggers target vulnerabilities**.

To address this issue, we propose replacing imprecise static-analysis-based distance metrics with vulnerability-oriented execution information to guide directed fuzzing. We call this framework trace-guided directed greybox fuzzing (TDGF). We refer to the execution information as a guidance trace, and we operationalize it as a seed-prioritization score: seeds whose executions overlap more with vulnerability-triggering behavior are scheduled earlier for mutation. Useful guidance traces should satisfy two requirements: (1) they provide reliable prioritization during fuzzing, and (2) they can be obtained or predicted with high accuracy. We conduct an empirical study of two

*Corresponding author.

representative forms of guidance traces: (1) vulnerability-reaching control flow and (2) the call stack at the vulnerability-triggering point. Our results show that, given ground-truth guidance traces, both substantially outperform prior static-analysis-based distance metrics. However, fine-grained control-flow traces do not yield the expected advantage, because small mutations can induce large and irregular changes in basic-block coverage, making control-flow traces **noisy** and **less reliable** for prioritization. In contrast, call-stack traces are **higher-level** and more **stable** under mutation-induced changes, providing a more reliable basis for ranking seeds. Moreover, motivated by the strong semantic and code-aware capabilities of large language models (LLMs), we investigate using LLMs to predict such guidance traces. The results show that call-stack prediction achieves an F1-score of over **0.70**, whereas control-flow prediction attains only about **0.20**, further supporting the practical advantage of call stacks.

Based on the TDGF framework, we present STACZZER, a framework that leverages LLMs to predict call stacks for guiding DGF. STACZZER first uses static analysis to construct the call graph (CG) and, based on the CG, identifies all methods that may reach the potential vulnerability location through a sequence of calls. If the source code of these methods is short, STACZZER submits it directly to the LLM in a single query to predict the call stack; otherwise, it uses code agents to query the codebase directly. This design maintains high call-stack prediction accuracy while significantly reducing the time overhead of code agents on small programs, and it also improves scalability when handling large codebases. Experimental results show that LLM-predicted call stacks achieve high accuracy, and the resulting acceleration of DGF closely matches the setting where the ground-truth call stacks are known. As LLM capabilities continue to advance, DGF is expected to benefit from increasingly accurate call-stack predictions on more complex programs.

We have implemented STACZZER on top of the greybox fuzzing framework AFL [42], and compared it against the following fuzzers: (1) AFLGo [5], the first DGF tool, which employs complex CFG-based distance metrics; (2) WINDRANGER [11], an optimized DGF tool that builds upon AFLGo by computing only deviation basic blocks (DBBs); (3) DAFL [19], the state-of-the-art (SOTA) DGF tool that leverages complex VFG-based distance metrics; (4) G²FUZZ [43], the SOTA CGF tool that leverages LLM-generated inputs; (5) AFL [42], the base framework for all fuzzers used in our evaluation. We use the same set of 41 real-world known vulnerabilities and the same evaluation metrics as in the experiments of the SOTA DGF tool DAFL. The total experimental time is approximately 58.4 CPU-years. The results show that STACZZER triggers vulnerabilities on average 2.13× to 3.14× faster than these baselines. Furthermore, by performing directed testing on existing patch locations in the latest versions of controlled experiment benchmarks, STACZZER successfully discovered 10 new vulnerabilities and 2 incomplete fixes in high-impact software GNU linker and its related Binutils components, with 10 assigned CVE IDs.

Contributions. This paper makes the following contributions:

- (1) We propose trace-guided directed greybox fuzzing to address the imprecision of conventional DGF static-analysis-based distance metrics.
- (2) We conduct an empirical study of two representative types of guidance traces. Counterintuitively, the results show that fine-grained vulnerability-triggering control-flow traces are not a practical choice, whereas call-stack traces are more effective.
- (3) We present STACZZER, a framework that integrates LLM-based prediction of vulnerability-triggering call stacks to guide DGF.
- (4) We show the effectiveness of STACZZER on a suite of real-world programs. STACZZER demonstrates significantly stronger vulnerability triggering performance compared to the baselines.

```

1  char** output;
2
3  void gnu_special(const char** mangled){
4      if('0' <= **mangled && **mangled <= '9'){
5          int n = 0;
6          while('0' <= **mangled && **mangled <= '9'){
7              n *= 10;
8              n += **mangled - '0';
9              (*mangled)++;
10         }
11         memcpy(*output, *mangled, n); // CVE-2016-4489
12     }
13     ...
14 }
15
16 void internal_cplus_demangle(const char** mangled,
17     bool flag){
18     if(flag){
19         if(**mangled != '\\0'){
20             memcpy(*output, "cplus_marker", 12);
21             (*output) += 12;
22             gnu_special(mangled);
23         }else{
24             if(strlen(*mangled) >= 9 && strcmp(*mangled, "
                _GLOBAL_", 8) == 0 && !('0' <= (*mangled)
                [8] && (*mangled)[8] <= '9')){
25                 (*mangled) += 8;
26                 gnu_special(mangled);
27             }
28         }
29     }
30 }
31
32 int main(){
33     const char** mangled = input1();
34     bool flag = input2();
35     internal_cplus_demangle(mangled, flag);
36     ...
37 }

```

Fig. 1. Simplified code fragment from `cxxfilt` containing CVE-2016-4489.Table 1. Information of two seeds s_0 and s_1 .

Seed	input1	input2
s_0	Alice	true
s_1	_GLOBAL_Bob	false

2 Motivating Example

In this section, using CVE-2016-4489 [28] in `cxxfilt` as a case study, we show that existing DGF methods use imprecise distance metrics to estimate a seed’s mutation potential toward the target, and we then show how our approach addresses this limitation.

2.1 A Seed Prioritization Problem in Directed Greybox Fuzzing

Figure 1 shows simplified `cxxfilt` code for CVE-2016-4489; we modified it for brevity while preserving vulnerability-relevant semantics. `cxxfilt` demangles C++ symbols by reversing compiler name mangling into human-readable form. From Line 33, the code reads the mangled input via `input1` into `mangled`, reads a boolean `flag` via `input2` at Line 34 to steer later control flow, and then calls `internal_cplus_demangle` with both parameters at Line 35 to start demangling. In this function, the code checks `flag` at Line 17 to choose between two branches, which we describe next:

- (1) If `flag` is true, the code checks at Line 18 whether `mangled` is empty; if not, it parses the input, writes to the output buffer (allocated at Line 1) at Line 19, advances the buffer pointer at Line 20, and calls `gnu_special` at Line 21.
- (2) If `flag` is false, the code checks at Line 24 whether `mangled` starts with `_GLOBAL_` and the next character is not a digit; if so, it finishes parsing `_GLOBAL_`, advances `mangled` at Line 25, and calls `gnu_special` at Line 26.

In `gnu_special`, the code checks at Line 4 whether `mangled` starts with a digit; if so, it parses consecutive digits into `n` from Line 5 to Line 9, and then copies `n` characters from `mangled` to the output buffer at Line 11. Because `n` is not range-checked, it can become huge or overflow negative, causing a segmentation fault at Line 11 and thus CVE-2016-4489.

DGF currently has two seeds, s_0 and s_1 , and must decide which to mutate first. As shown in Table 1, neither seed can directly trigger the vulnerability because input1 in both cases contains no digits. However, s_0 sets input2 to true while s_1 sets it to false. If input2 stays false, the vulnerability cannot be reached: `internal_cplus_demangle` takes its second branch, and the check in Line 24 ensures that the first character seen by Line 4 is not a digit, so the code at Line 11 is unreachable. Therefore, s_0 deserves higher mutation priority: it only needs to mutate the start of input1 into a large number, whereas s_1 must also flip input2 to true. The next subsection shows how existing imprecise distance metrics fail on this seed prioritization task.

2.2 Limitations of Existing Approaches with Imprecise Score Metrics

We analyze three DGF approaches that rely on imprecise distance metrics, namely AFLGo [5], WINDRANGER [11], and DAFL [19], showing that they can mis-prioritize seeds in the above case. These methods derive distances from static analysis and use them for seed prioritization, so they may be misled by control-flow or data-flow relations that do not occur in real vulnerability-triggering executions. Although they use different metrics, all of them depend directly on static analysis, which cannot be fully accurate [33]. Moreover, DGF typically compiles each software version separately, so heavy static analysis is too costly; many tools therefore use lightweight, coarse-grained analysis, which produces more imprecision and further aggravates the problem.

We first show how AFLGo [5] handles this case. For each seed execution, AFLGo collects the traversed CFG nodes and computes the harmonic mean of their shortest-path distances to the target statement, as shown in Figure 2. For simplicity, we treat each statement as its own basic block. Seeds with smaller average distances are considered easier to mutate into vulnerability-triggering inputs and are therefore prioritized. Under this scoring rule, the scores of s_0 and s_1 are computed as follows:

$$\begin{aligned} \text{SCORE}_{\text{AFLGo}}(s_0) &= 9 \left(\overbrace{10^{-1}}^{\text{Node 33}} + \overbrace{9^{-1}}^{\text{Node 34}} + \overbrace{8^{-1}}^{\text{Node 35}} + \overbrace{7^{-1}}^{\text{Node 17}} + \overbrace{7^{-1}}^{\text{Node 18}} + \overbrace{6^{-1}}^{\text{Node 19}} + \overbrace{5^{-1}}^{\text{Node 20}} + \overbrace{4^{-1}}^{\text{Node 21}} + \overbrace{3^{-1}}^{\text{Node 4}} \right)^{-1} \approx 5.75 \\ \text{SCORE}_{\text{AFLGo}}(s_1) &= 8 \left(\overbrace{10^{-1}}^{\text{Node 33}} + \overbrace{9^{-1}}^{\text{Node 34}} + \overbrace{8^{-1}}^{\text{Node 35}} + \overbrace{7^{-1}}^{\text{Node 17}} + \overbrace{6^{-1}}^{\text{Node 24}} + \overbrace{5^{-1}}^{\text{Node 25}} + \overbrace{4^{-1}}^{\text{Node 26}} + \overbrace{3^{-1}}^{\text{Node 4}} \right)^{-1} \approx 5.64 \end{aligned}$$

Because $\text{SCORE}_{\text{AFLGo}}(s_0) > \text{SCORE}_{\text{AFLGo}}(s_1)$, AFLGo would prioritize mutating s_1 , which is incorrect and inefficient. This happens because the CFG includes control-flow edges that never appear in vulnerability-triggering executions. As a result, static analysis assigns shorter distances to nodes 24, 25, and 26, even though they cannot lead to the vulnerability, than to nodes 18, 19, and 20.

We next describe how WINDRANGER [11] addresses this case. WINDRANGER introduces deviation basic blocks (DBBs), which are CFG nodes that can reach the target but have outgoing edges to nodes that cannot. DBBs are shown with double borders in Figure 2. WINDRANGER argues that averaging distances over all executed nodes, as in AFLGo, is diluted by many irrelevant nodes; it therefore computes distances only from executed DBBs to the target and prioritizes seeds with smaller arithmetic means. Under this scoring rule, the scores of s_0 and s_1 are computed as follows:

$$\begin{aligned} \text{SCORE}_{\text{WINDRANGER}}(s_0) &= \frac{\overbrace{7}^{\text{Node 18}} + \overbrace{3}^{\text{Node 4}}}{2} = 5 \\ \text{SCORE}_{\text{WINDRANGER}}(s_1) &= \frac{\overbrace{6}^{\text{Node 24}} + \overbrace{3}^{\text{Node 4}}}{2} = 4.5 \end{aligned}$$

Because $\text{SCORE}_{\text{WINDRANGER}}(s_0) > \text{SCORE}_{\text{WINDRANGER}}(s_1)$, WINDRANGER would still prioritize mutating s_1 , which is incorrect and inefficient. Although WINDRANGER reduces dilution from irrelevant

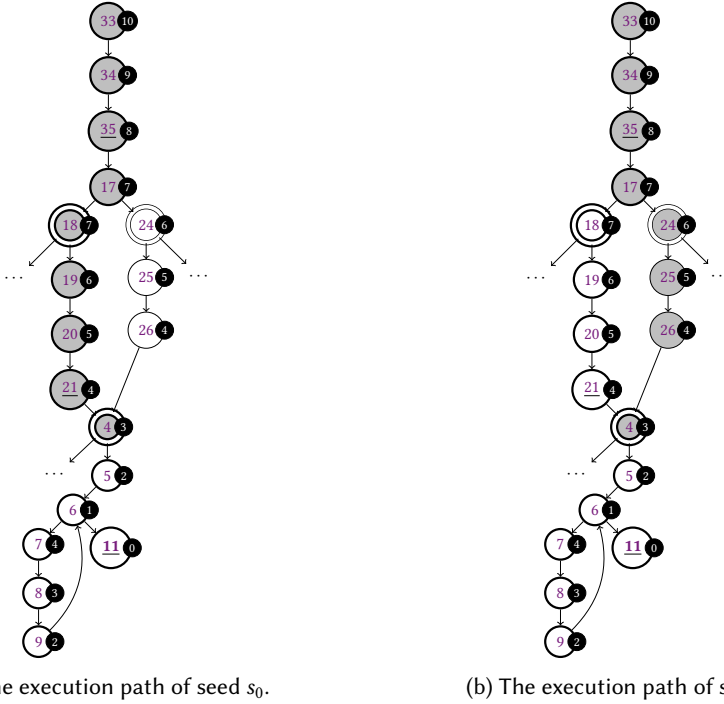


Fig. 2. CFG corresponding to the code fragment in Figure 1 and the nodes traversed by the execution paths of seeds s_0 and s_1 . For simplicity, each statement is treated as a separate basic block. The numbers within each node represent the line numbers in Figure 1, while the numbers in the small circles to the right of each node indicate their shortest distances to the target node. Nodes with gray backgrounds represent the nodes traversed by the seed’s execution path. Nodes with double borders represent deviation basic blocks (DBBs) as defined in WINDRANGER, which can reach the target node themselves but point to a node that cannot reach the target node. Nodes with bold numbers are target nodes. Nodes with bold borders belong to the ground-truth vulnerability-reaching control-flow trace, and nodes with underlined numbers belong to the ground-truth vulnerability-triggering call-stack trace.

nodes, it remains vulnerable to imprecise control-flow edges: DBB 24 cannot reach the target in vulnerability-triggering executions, but static analysis assigns it a smaller distance than DBB 18, leading to the wrong choice.

Finally, we show how DAFL [19] handles this case. DAFL argues that CFG-based control-flow feedback is too imprecise, and therefore uses a value-flow graph (VFG), whose edges represent potential data flows and thus exclude many useless edges compared to a CFG. For each seed execution, DAFL collects the traversed VFG nodes, as shown in Figure 3, and prioritizes seeds based on their shortest distances to the target statement. Let L be the maximum distance from any node to the target ($L = 3$ in our example). A node at distance i receives score $L - i + 1$, and DAFL prefers seeds with larger total scores over traversed nodes. Under this scoring rule, the scores of s_0 and s_1 are computed as follows:

$$\begin{aligned}
 \text{SCORE}_{\text{DAFL}}(s_0) &= \underbrace{L - 3 + 1}_{\text{Node 33}} + \underbrace{L - 2 + 1}_{\text{Node 35}} + \underbrace{L - 1 + 1}_{\text{Node 21}} = 6 \\
 \text{SCORE}_{\text{DAFL}}(s_1) &= \underbrace{L - 3 + 1}_{\text{Node 33}} + \underbrace{L - 2 + 1}_{\text{Node 35}} + \underbrace{L - 2 + 1}_{\text{Node 25}} + \underbrace{L - 1 + 1}_{\text{Node 26}} = 8
 \end{aligned}$$

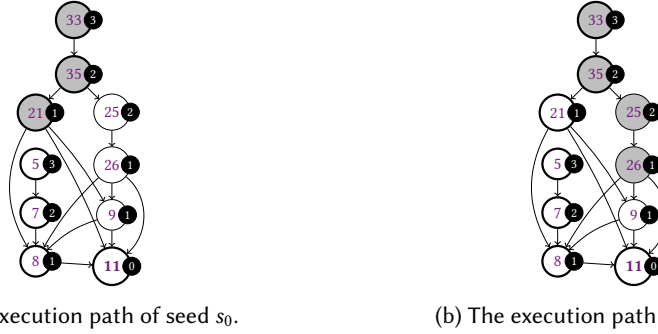
(a) The execution path of seed s_0 .(b) The execution path of seed s_1 .

Fig. 3. VFG for the code in Figure 1, highlighting the execution paths of seeds s_0 and s_1 . Node labels are line numbers in Figure 1. The numbers in the small circles to the right of each node indicate their shortest distances to the target node. Gray nodes are traversed by the seeds; bold numbers mark targets. Bold-bordered nodes lie on the ground-truth vulnerability-reaching value-flow trace.

Because $\text{SCORE}_{\text{DAFL}}(s_0) < \text{SCORE}_{\text{DAFL}}(s_1)$, DAFL would prioritize mutating s_1 , making the same incorrect choice as AFLGO and WINDRANGER. Although the VFG removes many meaningless CFG edges, it is still produced by static analysis and thus remains imprecise, so it can include data flows that never occur in real vulnerability-triggering executions. In our case, nodes 25 and 26 are mistakenly treated as having data flows that can reach the target, which inflates the score of s_1 .

In summary, we have demonstrated the limitations of three current DGF approaches that use imprecise distance metrics. To address this issue, we need to find more precise information beyond static analysis to guide DGF in seed prioritization.

2.3 Our Approach

We propose trace-guided directed greybox fuzzing (TDGF), which uses execution information that triggers the target vulnerability as a guidance trace to prioritize seeds. By abandoning imprecise static-analysis-based distance metrics, TDGF effectively avoids the misleading guidance caused by over-approximation. TDGF can leverage any type of execution information collected at vulnerability triggering time; in this work, we empirically study two representative trace types: (1) fine-grained vulnerability-reaching control flow and (2) coarse-grained call stacks at the vulnerability-triggering point. We detail this empirical study in Section 4. Below, we explain how TDGF instantiated with these two traces addresses the seed-prioritization problem in our case study.

We illustrate the two types of guidance traces in our case study:

$$\text{TRACE}_{\text{ControlFlow}} = \{33, 34, 35, 17, 18, 19, 20, 21, 4, 5, 6, 7, 8, 9, 11\} \quad \text{TRACE}_{\text{CallStack}} = \{35, 21, 11\}$$

We model each trace as a set because, for efficiency, greybox fuzzing [42] does not record the exact order or frequency of executed basic blocks; instead, it buckets this information. As a result, we can only tell whether a basic block was executed, so representing the guidance trace as a set makes the following computations more intuitive. In Figure 2, we draw nodes in $\text{TRACE}_{\text{ControlFlow}}$ with bold borders and mark nodes in $\text{TRACE}_{\text{CallStack}}$ by underlining their node numbers. $\text{TRACE}_{\text{ControlFlow}}$ includes all basic blocks executed in the vulnerability-triggering run, whereas $\text{TRACE}_{\text{CallStack}}$ includes the triggering basic block and the call sites on the call stack at that point.

TDGF computes, for each seed, the size of the intersection between its execution trace and the guidance trace. TDGF then prioritizes seeds with larger intersections for mutation. The intuition is that such seeds align more closely with the guidance trace and thus have a higher potential to

mutate into inputs that trigger the target vulnerability. The results are as follows:

$$\begin{aligned} \text{SCORE}_{\text{TRACE}_{\text{ControlFlow}}}(s_0) &= |\{33, 34, 35, 17, 18, 19, 20, 21, 4\} \cap \text{TRACE}_{\text{ControlFlow}}| = 9 \\ \text{SCORE}_{\text{TRACE}_{\text{ControlFlow}}}(s_1) &= |\{33, 34, 35, 17, 24, 25, 26, 4\} \cap \text{TRACE}_{\text{ControlFlow}}| = 5 \\ \text{SCORE}_{\text{TRACE}_{\text{CallStack}}}(s_0) &= |\{33, 34, 35, 17, 18, 19, 20, 21, 4\} \cap \text{TRACE}_{\text{CallStack}}| = 2 \\ \text{SCORE}_{\text{TRACE}_{\text{CallStack}}}(s_1) &= |\{33, 34, 35, 17, 24, 25, 26, 4\} \cap \text{TRACE}_{\text{CallStack}}| = 1 \end{aligned}$$

Since $\text{SCORE}_{\text{TRACE}_{\text{ControlFlow}}}(s_0) > \text{SCORE}_{\text{TRACE}_{\text{ControlFlow}}}(s_1)$ and $\text{SCORE}_{\text{TRACE}_{\text{CallStack}}}(s_0) > \text{SCORE}_{\text{TRACE}_{\text{CallStack}}}(s_1)$, TDGF prioritizes mutating s_0 under both types of guidance traces. TDGF makes the correct choice because it is not misled by imprecise static-analysis information.

To deploy TDGF in practice, we must choose a guidance-trace type. Fine-grained control-flow traces can intuitively provide stronger guidance than coarse-grained call stacks, but guidance traces are not available in advance; a practical option is to predict them with LLMs, and call-stack traces are plausibly easier for LLMs to predict than control-flow traces. We therefore need a systematic empirical study to understand this trade-off and make an informed design choice. We formalize **the proposed TDGF framework** in Section 3, then **empirically compare the two trace types** in Section 4, and finally propose STACZZER **based on TDGF and the study results** in Section 5.

3 The Trace-Guided Directed Greybox Fuzzing Framework

We first present some preliminaries, and then introduce our method.

3.1 Preliminaries

For the program to be fuzzed, we provide the following formal definitions for the relevant content.

Definition 3.1 (program input). We define \mathbf{S} as the set of program inputs. Each $s \in \mathbf{S}$ represents a possible input to the program.

Definition 3.2 (basic block). We define \mathbf{B} as the set of basic blocks. Each $b \in \mathbf{B}$ represents a specific basic block in the program.

Note that, in the example shown in Section 2, we treat each statement as a separate basic block for simplicity. In our experiments, basic blocks follow the standard definition, i.e., a straight-line sequence of instructions.

Definition 3.3 (crashing input). A crashing input $s \in \mathbf{S}$ refers to an input that causes the program to crash at basic block $b \in \mathbf{B}$ when executed with this input. We use a function $\text{CRASHING}(s, b) : \mathbf{S} \times \mathbf{B} \rightarrow \{\text{true}, \text{false}\}$ to represent whether input s causes the program to crash at basic block b .

Definition 3.4 (execution trace). The execution trace of an input $s \in \mathbf{S}$ refers to all basic blocks traversed when the program runs with this input. We use a function $\text{EXECUTION}(s) : \mathbf{S} \rightarrow \mathcal{P}(\mathbf{B})$ to represent the set.

Here, an execution trace is defined as a set of basic blocks because, in greybox fuzzing [42], the order and frequency with which a seed executes basic blocks are coarsened by bucketing for efficiency. Under this design, we can only determine whether a seed has executed a given basic block. We follow this design throughout. Therefore, in this paper, we define a seed’s execution trace as the set of basic blocks it traverses.

Definition 3.5 (goal of directed greybox fuzzing). The goal of directed greybox fuzzing is to generate an input $s \in \mathbf{S}$ such that $\text{CRASHING}(s, b_{\text{target}}) = \text{true}$ for a given target location $b_{\text{target}} \in \mathbf{B}$ in the shortest possible time.

Algorithm 1 Trace-guided directed greybox fuzzing.

Input: The set of initial seeds S_0 , the target basic block b_{target} , and the guidance trace GUIDANCE.

Output: The crashing seeds set S_\times .

```

1: procedure TDGF( $S_0, b_{\text{target}}, \text{GUIDANCE}$ )
2:    $S \leftarrow S_0, S_\times \leftarrow \emptyset$ 
3:   repeat
4:      $s \leftarrow \text{CHOOSESEED}(S, \text{GUIDANCE})$ 
5:      $e \leftarrow \text{ASSIGNENERGY}(S, s, \text{GUIDANCE})$ 
6:     for  $i = 1 \rightarrow e$  do
7:        $s' \leftarrow \text{MUTATE}(s)$ 
8:       if  $\text{EXECUTION}(s') \notin \{\text{EXECUTION}(s) \mid s \in S\}$  then
9:          $S \leftarrow S \cup \{s'\}$ 
10:      if  $\exists b \in \mathbf{B}$  such that  $\text{CRASHING}(s, b) = \text{true}$  then
11:         $S_\times \leftarrow S_\times \cup \{s'\}$ 
12:   until timeout
13:   return  $S_\times$ 

```

3.2 Overview

[Algorithm 1](#) formalizes the workflow of trace-guided directed greybox fuzzing (TDGF), extending the greybox fuzzer AFL [42]. The two AFL-specific lines ([Line 4](#) and [Line 5](#)) modified in TDGF are highlighted in gray: (1) AFL’s CHOOSESEED selects a seed for prioritization; we instead prioritize seeds whose execution paths overlap more with the guidance traces. (2) AFL’s ASSIGNENERGY assigns mutation energy to the selected seed; we instead allocate more energy to seeds with higher overlap between their execution paths and the guidance traces. TDGF takes as input an initial seed set $S_0 \subseteq S$, a target program location $b_{\text{target}} \in \mathbf{B}$, and a *guidance trace* $\text{GUIDANCE} \subseteq \mathbf{B}$. TDGF outputs the set of crashing inputs S_\times . TDGF maintains a current seed set S (initialized to S_0) and a crashing set S_\times (initialized to empty) ([Line 2](#)), and then repeatedly performs the following fuzzing loop ([Line 3](#)):

- (1) TDGF selects a seed $s \in S$ to prioritize for mutation in the current round based on the guidance trace GUIDANCE ([Line 4](#), detailed in [Section 3.3](#)), and assigns it an energy value $e \in \mathbb{N}$ based on GUIDANCE ([Line 5](#), detailed in [Section 3.4](#)). Here, energy is the number of mutations performed in the round, following standard greybox fuzzing terminology [5, 6, 19]. Assigning energy is commonly called power scheduling [6]; higher energy means higher priority and more mutation time.
- (2) Given energy e , TDGF mutates seed s for e times ([Line 6](#)); each iteration calls $\text{MUTATE}(s)$ to produce a new seed s' ([Line 7](#)). $\text{MUTATE}(s)$ uses the same mutation settings as AFL [42], randomly choosing a mutator (for example, bit flips, byte-level add/subtract, deleting a random-length byte sequence, and so on).
- (3) If the execution trace of s' differs from that of all existing seeds ([Line 8](#)), TDGF keeps s' ([Line 9](#)); if s' crashes ([Line 10](#)), TDGF also adds it to S_\times ([Line 11](#)).

When the time budget is exhausted ([Line 12](#)), TDGF returns the set of crashing seeds S_\times ([Line 13](#)). TDGF aims to generate an s' ([Line 7](#)) such that $\text{CRASHING}(s', b_{\text{target}}) = \text{true}$ as quickly as possible.

3.3 Seed Selection

[Algorithm 2](#) formalizes TDGF’s seed-selection algorithm. The algorithm takes as input the current seed set $S \subseteq S$ and the guidance trace GUIDANCE. The algorithm outputs a seed $s \in S$ for priority mutation. TDGF maintains a global set S_{chosen} of seeds already mutated in the current round (initialized to empty) ([Line 1](#)). If all seeds in S have been mutated ([Line 3](#)), TDGF starts a new round

Algorithm 2 The algorithm to choose seed for mutation in TDGF.**Input:** The set of current seeds S , and the guidance trace GUIDANCE.**Output:** The seed for mutation s .

```

1:  $S_{\text{chosen}} \leftarrow \emptyset$ 
2: procedure CHOOSESEED( $S$ , GUIDANCE)
3:   if  $S_{\text{chosen}} = S$  then
4:      $S_{\text{chosen}} \leftarrow \emptyset$ 
5:    $S_{\text{current}} \leftarrow S - S_{\text{chosen}}$ 
6:    $s \leftarrow \arg \max_{s' \in S_{\text{current}}} \text{SCORE}(s', \text{GUIDANCE})$ 
7:    $S_{\text{chosen}} \leftarrow S_{\text{chosen}} \cup \{s\}$ 
8:   return  $s$ 

```

Algorithm 3 The algorithm to assign energy for the seed for mutation in TDGF.**Input:** The set of current seeds S , the seed for mutation s , and the guidance trace GUIDANCE.**Output:** The energy assigned to the seed for mutation e .

```

1: procedure ASSIGNEnergy( $S$ ,  $s$ , GUIDANCE)
2:    $\text{SCORE}_{\text{average}} \leftarrow \frac{\sum_{s' \in S} \text{SCORE}(s', \text{GUIDANCE})}{|S|}$ 
3:    $e \leftarrow \left\lceil \frac{\text{SCORE}(s, \text{GUIDANCE})}{\text{SCORE}_{\text{average}}} \cdot \text{ENERGY}_{\text{AFL}}(s) \right\rceil$ 
4:   return  $e$ 

```

by clearing S_{chosen} (Line 4). TDGF then forms S_{current} as the seeds not yet mutated in the current round (Line 5). For each $s' \in S_{\text{current}}$, TDGF computes the overlap score $\text{SCORE}(s', \text{GUIDANCE})$ between the execution trace of s' and GUIDANCE (Line 6), defined as follows:

$$\text{SCORE}(s', \text{GUIDANCE}) = |\text{EXECUTION}(s') \cap \text{GUIDANCE}|$$

TDGF selects the seed s with the largest overlap score for priority mutation, adds it to S_{chosen} (Line 7), and returns s (Line 8).

3.4 Power Scheduling

Algorithm 3 formalizes TDGF’s energy-assignment algorithm. The algorithm takes as input the current seed set $S \subseteq \mathbb{S}$, the selected seed $s \in S$, and the guidance trace GUIDANCE. The algorithm outputs an energy value $e \in \mathbb{N}$ for s . TDGF first computes the average overlap score $\text{SCORE}_{\text{average}}$ between the execution traces of all current seeds and GUIDANCE (Line 2). It then scales the baseline energy $\text{ENERGY}_{\text{AFL}}(s)$ that AFL [42] would assign to s by an adjustment factor (Line 3), defined as the ratio between s ’s overlap score and $\text{SCORE}_{\text{average}}$. Thus, seeds with higher overlap receive more energy. Here, $\text{ENERGY}_{\text{AFL}}(s)$ is AFL’s heuristic energy based on metrics such as execution time and trace length. TDGF finally returns the assigned energy e (Line 4).

4 Empirical Study

We empirically study two typical guidance traces observed when triggering a vulnerability, namely the control-flow trace and the call-stack trace, denoted as CONTROLFLOW and CALLSTACK, respectively. We expect that the results of this study will help us make an informed design choice when incorporating TDGF into our final framework, thereby improving the effectiveness of DGF in practical settings.

In particular, we aim to answer the following three questions:

- (1) How effective is TDGF when provided with ground-truth guidance traces?
- (2) As a fine-grained guidance trace, how much improvement does CONTROLFLOW offer compared to the coarse-grained CALLSTACK?

Table 2. Benchmarks used in the experiments. The **Type** column indicates the abbreviated type of each vulnerability: **BF** (Buffer Overflow), **NPD** (Null Pointer Dereference), **SO** (Stack Overflow), **UAF** (Use-After-Free), **IO** (Integer Overflow), **OOM** (Out-Of-Memory).

Project	Program	Version	CVE ID	Type	
Ming	swftophp	0.4.7	2016-9827	BO	
			2016-9829	NPD	
			2016-9831	BO	
			2017-9988	NPD	
			2017-11728	NPD	
			2017-11729	NPD	
			2017-7578	BO	
	0.4.8	2018-7868	UAF		
		2018-8807	UAF		
		2018-8962	UAF		
		2018-11095	UAF		
		2018-11225	BO		
		2018-11226	BO		
		2018-20427	NPD		
Lrzip	lrzip	0.631	2017-8846	UAF	
			2018-11496	UAF	
Binutils	cxxfilt	2.26	2016-4487	NPD	
			2016-4489	UAF	
Binutils	cxxfilt	2.26	2016-4490	IO	
			2016-4491	SO	
			2016-4492	IO	
			2016-6131	SO	
	objcopy	2.28	2017-8393	BO	
			2017-8394	NPD	
			2017-8395	NPD	
	objdump	2.28	2017-8392	NPD	
			2017-8396	BO	
			2017-8397	BO	
			2017-8398	BO	
			2.31.1	2018-17360	BO
			strip	2.27	2017-7303
	nm	2.29	2017-14940	OOM	
readelf	2.29	2017-16828	IO		
Libxml2	xmllint	2.9.4	2017-5969	NPD	
			2017-9047	BO	
			2017-9048	BO	
Libjpeg	cjpeg	2.0.4	2018-14498	BO	
			2020-13790	BO	

- (3) In practical engineering scenarios, how accurate are LLMs at predicting these two types of guidance traces?

We first describe the experimental setup in Section 4.1. We then answer the first two questions through experiments and analysis in Section 4.2. Finally, we address the third question in Section 4.3.

4.1 Experimental Setup

We run all experiments on Linux machines with 256 processors (2.25 GHz) and 256 GB RAM, and implement TDGF on top of AFL [42].

Baselines. We compare TDGF with: (1) AFLGo [5], which prioritizes seeds using CFG distances between execution traces and targets; (2) WINDRANGER [11], which refines AFLGo by computing distances only from deviation basic blocks to reduce interference from irrelevant blocks; (3) DAFL [19], a SOTA directed greybox fuzzer that prioritizes seeds using distances on a value-flow graph; and (4) AFL [42], the base fuzzer for both our approach and the other baselines.

Benchmarks. Table 2 lists our benchmarks, which include 41 known vulnerabilities from 10 programs. For each vulnerability, we report its CVE ID and type. We use the same benchmark as the SOTA DGF tool DAFL [19]. These vulnerabilities come from programs widely used in prior DGF work [7, 16, 19], so the benchmark spans diverse scenarios and provides a representative testbed for evaluating DGF techniques. We compile each program with AddressSanitizer [35], which reports a crash backtrace and lets us reliably determine whether an input triggers the target vulnerability.

Metrics. For each fuzzer and vulnerability, we run 40 trials to mitigate randomness from mutation and set a 24-hour time limit per trial, matching DAFL [19]. Each trial runs in a dedicated Docker container pinned to a dedicated CPU core. We record time-to-exposure (TTE), defined as the time until the first trigger of the vulnerability. Following DAFL, we use the median of the 40 TTEs. If at least 20 trials do not trigger within the time limit, the median is undefined, and we set it to a penalty value of twice the time limit (48 h). We say a vulnerability is stably reproducible by a fuzzer if and only if its median TTE is defined without the penalty. Consistent with DAFL, we include

Table 3. Summary of results for TDGF with two types of guidance metrics and each baseline over 40 runs on 41 known vulnerabilities. The **TDGF_T’s average speedup** row ($T \in \{\text{CONTROLFLOW}, \text{CALLSTACK}\}$) denotes the average speedup (in terms of median TTE) achieved by TDGF_T over the corresponding configuration across the 41 vulnerabilities. The **# Stably reproducible** row reports the number of vulnerabilities for which each fuzzer can compute a valid median TTE. In the **Performance vs. TDGF_T** row, a/b indicates that TDGF_T outperforms the fuzzer on a vulnerabilities while being outperformed on b vulnerabilities. This value is used to calculate the sign test p -value shown in the next row.

Metric	TDGF _{CONTROLFLOW}	TDGF _{CALLSTACK}	AFLGo	WINDRANGER	DAFL	AFL
TDGF _{CONTROLFLOW} ’s average speedup	-	1.23	3.47	2.99	2.08	2.47
TDGF _{CALLSTACK} ’s average speedup	-	-	3.30	2.51	2.14	2.16
# Stably reproducible	28	29	22	21	27	23
Performance vs. TDGF _{CONTROLFLOW}	-	20/16	32/4	27/9	28/10	25/11
P-value in the sign test	-	0.31	10^{-6}	0.002	0.003	0.01
Performance vs. TDGF _{CALLSTACK}	-	-	30/4	29/6	28/7	27/9
P-value in the sign test	-	-	3×10^{-6}	6×10^{-5}	3×10^{-4}	0.002

static-analysis overhead in TTE because directed fuzzing is often used for patch testing where each code change requires recompilation, so static analysis is not a one-time cost.

Guidance traces. For each vulnerability, we use its proof-of-concept (PoC) input to trigger a crash, record the executed basic-block set as GUIDANCE_{CONTROLFLOW}, and collect the crash backtrace to build GUIDANCE_{CALLSTACK} as the set of basic blocks on the reported call stack, including the basic block containing the crashing statement.

4.2 Effectiveness of TDGF with Ground-Truth Guidance Traces

We denote the TDGF configuration that uses GUIDANCE_{CONTROLFLOW} and GUIDANCE_{CALLSTACK} as guidance traces by TDGF_{CONTROLFLOW} and TDGF_{CALLSTACK}, respectively. Table 3 summarizes the results of TDGF_T ($T \in \{\text{CONTROLFLOW}, \text{CALLSTACK}\}$) and several baselines on 41 known vulnerabilities.

To answer question (1), we report the average speedup of TDGF_T over the baselines. TDGF_{CONTROLFLOW} achieves $2.08\times$ to $3.47\times$ speedups, and TDGF_{CALLSTACK} achieves $2.14\times$ to $3.30\times$. They stably reproduce 28 and 29 vulnerabilities, respectively, exceeding all baselines. We also report per-vulnerability win-loss results in the **Performance vs. TDGF_T** rows. For each vulnerability, we compare median TTE; if the median TTE is unavailable for both, we compare the number of successful triggers. Each result is written as a/b , where a is the number of cases where TDGF_T is better and b is the number of cases where the baseline is better. The win-loss ratios range from $2.27\times$ to $8\times$ for TDGF_{CONTROLFLOW} and from $3\times$ to $7.5\times$ for TDGF_{CALLSTACK}, highlighting the benefit of trace-guided fuzzing. Finally, we perform a one-tailed sign test [15], where a and b are the numbers of positive and negative signs, respectively; the p -values (shown in the subsequent **P-value in the sign test** rows) are all far below 0.05. **Therefore, our answer to question (1) is that TDGF_T significantly outperforms all baselines, and TDGF is effective with either type of ground-truth guidance trace.**

To answer question (2), we compare TDGF_{CONTROLFLOW} with TDGF_{CALLSTACK}. TDGF_{CONTROLFLOW} is only $1.23\times$ faster and stably reproduces one fewer vulnerability. In the win-loss comparison, it wins on 20 vulnerabilities and loses on 16, so neither trace type consistently dominates. Accordingly, the one-tailed sign test fails to reject the null hypothesis, and we cannot claim that TDGF_{CONTROLFLOW} significantly outperforms TDGF_{CALLSTACK}. Thus, although CONTROLFLOW is more fine-grained, it does not provide significantly stronger guidance than the coarser CALLSTACK. To explain this seemingly counter-intuitive result, we introduce triggering-seed mutation paths.

Definition 4.1 (Triggering-seed mutation path). Let s_{trigger} be the earliest input generated by the fuzzer such that $\text{CRASH}(s_{\text{trigger}}, b_{\text{target}}) = \text{true}$. Then there exists a unique triggering-seed mutation path (s_1, s_2, \dots, s_n) such that $s_1 \in S_0$, $s_n = s_{\text{trigger}}$, and for all $i \in \{2, \dots, n\}$, s_i is mutated from s_{i-1} .

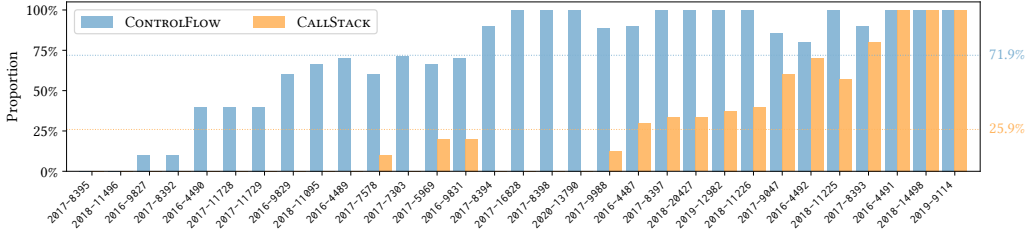


Fig. 4. The proportion of triggering-seed mutation paths whose scores are not monotonically non-decreasing. The dotted line represents the average value.

Ideally, along a triggering-seed mutation path (s_1, s_2, \dots, s_n) , the TDGF scores $\text{SCORE}(s_1, \text{GUIDANCE}_T)$, $\text{SCORE}(s_2, \text{GUIDANCE}_T), \dots, \text{SCORE}(s_n, \text{GUIDANCE}_T)$ should be monotonically non-decreasing, meaning that seeds move progressively closer to the target trace. Figure 4 reports, across all runs of $\text{TDGF}_{\text{CONTROLFLOW}}$ and $\text{TDGF}_{\text{CALLSTACK}}$, the fraction of triggering-seed mutation paths whose score sequences are **not** monotonically non-decreasing. For CONTROLFLOW , the average reaches 71.9%, while for CALLSTACK it is 25.9%. This suggests that under $\text{TDGF}_{\text{CONTROLFLOW}}$, seeds off the triggering path often receive higher scores than seeds on the path, whereas this happens much less frequently under $\text{TDGF}_{\text{CALLSTACK}}$. A plausible explanation is that CONTROLFLOW is too fine-grained: a single mutation may reduce control-flow overlap before increasing it again later, so progress is not smooth. The coarser CALLSTACK trace mitigates this effect because one mutation is less likely to change the call stack drastically. Consequently, the extra fine-grained information in CONTROLFLOW often behaves like noise: seeds that should be prioritized typically have higher call-stack overlap, but do not necessarily show higher control-flow overlap beyond that. Hence, CONTROLFLOW offers limited benefit over CALLSTACK for guidance. **Therefore, our answer to question (2) is that CONTROLFLOW does not provide significantly stronger guidance than CALLSTACK , due to its overly fine-grained nature.**

4.3 Accuracy of Guidance Trace Prediction in Practice

To answer question (3), we use two state-of-the-art code agents, Codex 0.75.0 [29] (GPT-5.1-codex-max high [31]) and Claude Code 2.0.76 [1] (Claude-Opus-4.5-20251101 [2]), to predict the two types of guidance traces. We set the temperature to the default value of 1.0. Figure 5 shows the prompt templates used; we query the code agents directly on each program’s codebase. For evaluation, we corrected the ground truth by removing line numbers that do not exist in the codebase (e.g., those from dynamically linked libraries). Table 4 reports the average accuracy under different metrics. Both code agents achieve very low accuracy on CONTROLFLOW : all three metrics are around 0.2. In contrast, the metrics for CALLSTACK are all above 0.7. This aligns with intuition: CALLSTACK is more general and coarse-grained, which LLMs tend to handle well, whereas CONTROLFLOW is fine-grained and requires rigorous logical reasoning, making it much harder for LLMs. **Therefore, in response to question (3), we conclude that CALLSTACK is easier to predict than CONTROLFLOW .**

Based on our answers to the three questions, we conclude that CALLSTACK provides nearly the same guidance capability as CONTROLFLOW , yet is substantially easier for LLMs to predict, making it a more suitable guidance trace for TDGF. Motivated by this observation, we propose STACZZER, a framework that guides directed greybox fuzzing using LLM-predicted vulnerability-triggering call stacks. We introduce STACZZER in the next section.

<p>System: You are a fuzzing expert, well-versed in the operation logic of AFL and its extension tools. You have a deep understanding of bugs inherent in the code.</p>	
<p>Prompt Content for CONTROLFLOW: In the current codebase, there may exist an input originating from the <MAIN> entry point that triggers a vulnerability in <TARGET>. Please identify the corresponding execution path and output every line of code executed along this path based on your code understanding and static reasoning.</p>	<p>Prompt Content for CALLSTACK: In the current codebase, there may exist an input originating from the <MAIN> entry point that triggers a vulnerability in <TARGET>. Please output the possible call stack that would directly trigger the crash (that is, if there were a sanitizer report) based on your code understanding and static reasoning.</p>

Fig. 5. Prompt template for instructing the LLM to predict guidance traces. For brevity, formatting details and examples are omitted.

Table 4. Average accuracy of guidance traces prediction using the code agents.

Type	Codex			Claude Code		
	Precision	Recall	F1-Score	Precision	Recall	F1-Score
CONTROLFLOW	0.272	0.248	0.209	0.242	0.174	0.174
CALLSTACK	0.766	0.719	0.730	0.748	0.709	0.718

Algorithm 4 The STACZZER framework.

Input: The set of initial seeds S_0 and the target basic block b_{target} .

Output: The crashing seeds set S_x .

```

1: procedure STACZZER( $S_0, b_{\text{target}}$ )
2:   SLICE  $\leftarrow$  All function slices reaching the function containing  $b_{\text{target}}$  on the call graph
3:   if Token count of SLICE  $\leq 10^5$  then
4:     GUIDANCEPREDICTEDCALLSTACK  $\leftarrow$  SINGLETURNPREDICTION()
5:   else
6:     GUIDANCEPREDICTEDCALLSTACK  $\leftarrow$  CODEAGENTPREDICTION()
7:   return TDGF( $S_0, b_{\text{target}}, \text{GUIDANCE}_{\text{PREDICTEDCALLSTACK}}$ )

```

5 The STACZZER Framework

Algorithm 4 formalizes the workflow of the STACZZER framework. STACZZER follows the TDGF paradigm and uses LLM-predicted call stacks as the guidance trace. Given an initial seed set S_0 and a target program location b_{target} , STACZZER outputs the set of inputs that can trigger program crashes, denoted as S_x .

In practice, DGF is typically applied to a specific software version; each code update requires recompilation and reprocessing, so the preprocessing cost is not a one-time overhead [19]. With this in mind, STACZZER first performs static analysis to build the call graph, and then collects function-level slices for all functions that can reach the target function in the call graph (Line 2). If the slice is small enough in terms of token count (Line 3), STACZZER directly feeds it to an LLM in a single turn to predict call stacks (Line 4); otherwise, STACZZER uses a code agent to perform the prediction (Line 6). This design has two benefits:

- (1) For small programs, code agents can be overly time-consuming. For some vulnerabilities, the cost can even exceed fuzzing itself. When the function slice is sufficiently small, single-turn LLM prediction makes the LLM overhead negligible. STACZZER sets the token threshold to 10^5 to ensure prediction accuracy.
- (2) For large programs, the relative overhead of using a code agent becomes less significant. Thus, we use code agents to improve prediction accuracy while maintaining scalability to large codebases.

Table 5. Median TTE (including preprocessing) over 40 runs on 41 known vulnerabilities. **MTTE** is the median TTE (s); if unavailable, we report $(x/40)$ where x runs trigger the bug. **Ratio** is the MTTE relative to STACZZER; if MTTE is unavailable, it is computed using $2\times$ the time limit (48h). The best fuzzer per vulnerability is in bold. In **Performance vs. STACZZER**, a/b means STACZZER wins on a vulnerabilities and loses on b ; this is used for the sign-test p-value shown in the next row. **# Stably reproducible** counts vulnerabilities with a computable MTTE, and **# Best performance** counts vulnerabilities where each fuzzer is best.

Program	CVE ID	STACZZER		AFLGo		WINDRANGER		DAFL		G ² Fuzz		AFL	
		MTTE	Ratio	MTTE	Ratio	MTTE	Ratio	MTTE	Ratio	MTTE	Ratio	MTTE	Ratio
swftophp	2016-9827	112	461	4.12	95	0.85	147	1.31	123	1.10	116	1.04	
	2016-9829	245	676	2.76	501	2.04	411	1.68	466	1.90	429	1.75	
	2016-9831	526	785	1.49	459	0.87	315	0.60	607	1.15	416	0.79	
	2017-9988	4,704	3,925	0.83	3,395	0.72	4,101	0.87	4,548	0.97	3,473	0.74	
	2017-11728	599	2,815	4.70	995	1.66	631	1.05	3,231	5.39	2,364	3.95	
	2017-11729	213	978	4.59	400	1.88	287	1.35	1,196	5.62	826	3.88	
	2017-7578	416	845	2.03	680	1.63	643	1.55	333	0.80	848	2.04	
	2018-7868	(1/40)	(0/40)	1.00	(0/40)	1.00	(12/40)	1.00	(0/40)	1.00	(0/40)	1.00	
	2018-8807	(0/40)	(0/40)	1.00	(0/40)	1.00	(0/40)	1.00	(0/40)	1.00	(0/40)	1.00	
	2018-8962	(0/40)	(0/40)	1.00	(0/40)	1.00	(2/40)	1.00	(0/40)	1.00	(0/40)	1.00	
	2018-11095	837	8,339	9.96	2,949	3.52	2,699	3.22	5,542	6.62	6,873	8.21	
	2018-11225	32,673	(8/40)	5.29	(11/40)	5.29	45,296	1.39	(17/40)	5.29	(13/40)	5.29	
	2018-11226	79,229	(11/40)	2.18	(11/40)	2.18	62,402	0.79	(10/40)	2.18	(11/40)	2.18	
	2018-20427	(18/40)	11,154	0.06	(11/40)	1.00	24,395	0.14	14,293	0.08	9,846	0.06	
	2019-9114	51,070	(20/40)	3.38	(16/40)	3.38	(8/40)	3.38	83,770	1.64	(15/40)	3.38	
	2019-12982	40,420	(14/40)	4.28	(13/40)	4.28	71,703	1.77	51,079	1.26	(18/40)	4.28	
2020-6628	47,681	(10/40)	3.62	(4/40)	3.62	(15/40)	3.62	(9/40)	3.62	(17/40)	3.62		
lrzip	2017-8846	(2/40)	(1/40)	1.00	(0/40)	1.00	(1/40)	1.00	(0/40)	1.00	(0/40)	1.00	
	2018-11496	23	193	8.39	21	0.91	25	1.09	21	0.91	35	1.52	
cxxfilt	2016-4487	655	1,083	1.65	2,408	3.68	574	0.88	1,000	1.53	862	1.32	
	2016-4489	502	2,628	5.24	790	1.57	2,235	4.45	2,570	5.12	1,871	3.73	
	2016-4490	205	804	3.92	620	3.02	1,080	5.27	594	2.90	618	3.01	
	2016-4491	(0/40)	(1/40)	1.00	(0/40)	1.00	(4/40)	1.00	(1/40)	1.00	(0/40)	1.00	
	2016-4492	3,016	3,566	1.18	5,272	1.75	3,944	1.31	6,337	2.10	3,210	1.06	
	2016-6131	(0/40)	(1/40)	1.00	(0/40)	1.00	(0/40)	1.00	(0/40)	1.00	(0/40)	1.00	
objcopy	2017-8393	860	4,417	5.14	3,090	3.59	1,977	2.30	3,740	4.35	3,415	3.97	
	2017-8394	641	3,563	5.56	1,268	1.98	15,029	23.45	2,862	4.46	1,367	2.13	
	2017-8395	506	1,857	3.67	221	0.44	290	0.57	251	0.50	194	0.38	
objdump	2017-8392	326	2,209	6.78	629	1.93	361	1.11	439	1.35	466	1.43	
	2017-8396	(0/40)	(0/40)	1.00	(1/40)	1.00	(0/40)	1.00	(2/40)	1.00	(1/40)	1.00	
	2017-8397	77,803	(17/40)	2.22	(18/40)	2.22	(7/40)	2.22	(10/40)	2.22	84,774	1.09	
	2017-8398	8,535	6,253	0.73	2,897	0.34	4,834	0.57	6,936	0.81	5,822	0.68	
2018-17360	(1/40)	(0/40)	1.00	(0/40)	1.00	(0/40)	1.00	(0/40)	1.00	(4/40)	1.00		
strip	2017-7303	663	3,805	5.74	5,708	8.61	667	1.01	261	0.39	233	0.35	
nm	2017-14940	(0/40)	(0/40)	1.00	(0/40)	1.00	(0/40)	1.00	(0/40)	1.00	(0/40)	1.00	
readelf	2017-16828	303	1,139	3.76	816	2.69	1,723	5.69	1,148	3.79	628	2.07	
xmllint	2017-5969	1,089	3,166	2.91	4,647	4.27	1,410	1.29	683	0.63	665	0.61	
	2017-9047	69,109	(5/40)	2.50	(2/40)	2.50	(13/40)	2.50	(4/40)	2.50	(5/40)	2.50	
	2017-9048	18,843	(1/40)	9.17	(1/40)	9.17	13,093	0.69	(5/40)	9.17	(4/40)	9.17	
cjpeg	2018-14498	(8/40)	(2/40)	1.00	(0/40)	1.00	23,156	0.13	(14/40)	1.00	(11/40)	1.00	
	2020-13790	(6/40)	(1/40)	1.00	(4/40)	1.00	(6/40)	1.00	(1/40)	1.00	(2/40)	1.00	
Average speedup		-	3.14		2.26		2.13		2.23		2.13		
Performance vs. STACZZER		-	32/5		29/7		24/12		26/11		26/10		
P-value in the sign test		-	4×10^{-6}		2×10^{-4}		0.03		0.01		0.006		
# Stably reproducible		29	22		21		27		24		23		
# Best performance		19	1		4		9		3		5		

the effectiveness of STACZZER. The p-values from the one-tailed sign test based on win-loss counts are all below 0.05, indicating that STACZZER significantly outperforms all baselines. STACZZER can stably reproduce 29 vulnerabilities, outperforming all other baselines. Moreover, the **# Best performance** row shows that STACZZER achieves the best performance on 19 vulnerabilities, which is $2.11\times$ to $19\times$ that of other baselines.

We further show in [Figure 7](#) the token counts of call-graph-reachable function slices in STACZZER. For most vulnerabilities, slices stay within our 10^5 -token limit; only four exceed it. In [Table 6](#), we

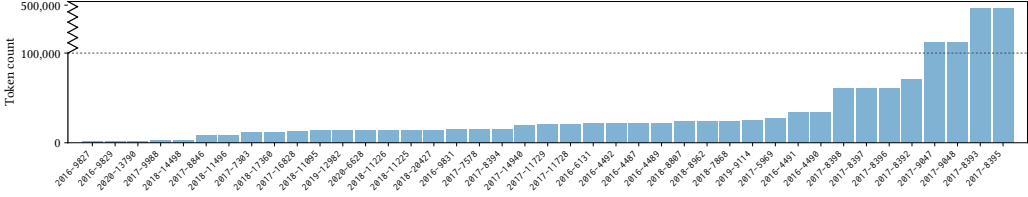


Fig. 7. Token counts of function slices in the call graph that can reach the target for the 41 vulnerabilities.

Table 6. Token count and time overhead of the code agent prediction on the remaining 4 vulnerabilities.

Metric	2017-8393	2017-8395	2017-9047	2017-9048
Token count	1,462,307	999,598	2,297,026	1,611,668
Time overhead (s)	260	233	303	177

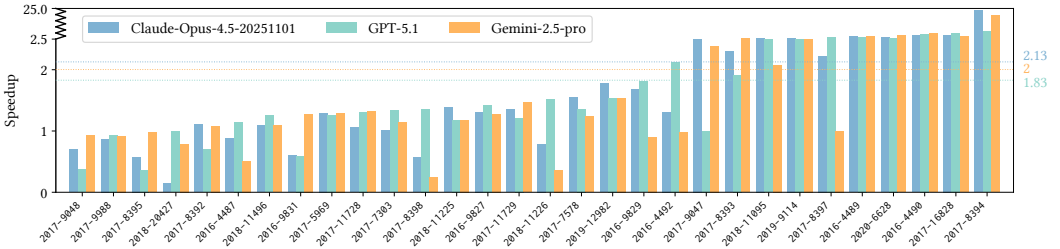


Fig. 8. Speedup over DAFL under different LLM settings. The dotted line represents the average value. For brevity, vulnerabilities that no fuzzer can stably reproduce are omitted.

report the code-agent token and time overhead for these four cases. Overall, STACZZER’s LLM token and time costs are acceptable.

Overall, STACZZER attains high accuracy in call-stack prediction, thereby providing strong acceleration for DGF.

6.3 Impact of Different LLMs

We additionally evaluated two representative LLMs: (1) GPT-5.1 [30] for SINGLETURNPREDICTION and Codex 0.75.0 [29] (GPT-5.1-codex-max high [31]) for CODEAGENTPREDICTION; (2) Gemini-2.5-pro [13] for SINGLETURNPREDICTION and Gemini CLI 0.25.2 [14] (Gemini-2.5-pro [13]) for CODEAGENTPREDICTION. We set the temperature to its default value of 1.0. GPT-5.1 and Gemini-2.5-pro achieve average (Precision, Recall, F1) scores of (0.750, 0.694, 0.714) and (0.716, 0.705, 0.701), respectively. Figure 8 reports the speedup of STACZZER over the state-of-the-art directed greybox fuzzer DAFL when instantiated with three different LLMs. The average speedup ranges from $1.83\times$ to $2.13\times$; all three variants substantially outperform the baseline and exhibit no significant differences. **These results indicate that STACZZER is not tied to a specific LLM, but achieves strong performance across diverse LLM backends.**

6.4 Ablation Study

We conduct an ablation study on the components of STACZZER: (1) SEEDPOOL denotes enabling only seed selection, i.e., we do not modify Line 5 and instead use AFL’s original power-scheduling strategy; (2) ENERGY denotes enabling only power scheduling, i.e., we do not modify Line 4 and instead use AFL’s original seed-selection strategy; and (3) CALLGRAPH denotes using all call sites

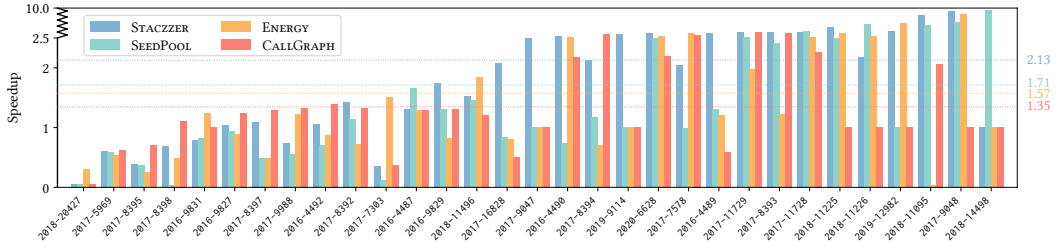


Fig. 9. Speedup over AFL under different ablation settings. The dotted line represents the average value. For brevity, vulnerabilities that no fuzzer can stably reproduce are omitted.

Table 7. New bugs found through regression patch testing on the latest versions of benchmarks from the controlled experiments.

Program	Location	CWE	CVE
objdump	objdump.c:4501	Out-of-bounds Read	CVE-2025-11081
	prdbg.c:2452	Unexpected Status Code or Return Value	CVE-2025-11839
ld	elf-eh-frame.c:756	Heap-based Buffer Overflow	CVE-2025-11082
	cache.c:435	Heap-based Buffer Overflow	CVE-2025-11083
	elflink.c:14898	Out-of-bounds Read	CVE-2025-11412
	libbfd.c:989	Heap-based Buffer Overflow	CVE-2025-11413
	elflink.c:115	Out-of-bounds Read	CVE-2025-11414
	elf-eh-frame.c:2170	Out-of-bounds Read	CVE-2025-11494
	elf64-x86-64.c:4507	Heap-based Buffer Overflow	CVE-2025-11495
ldmisc.c:527	Out-of-bounds Read	CVE-2025-11840	

Table 8. Incomplete fixes discovered through incremental patch testing on the patched versions of newly found vulnerabilities in Table 7.

Program	Location	CWE	Original CVE
ld	elf-eh-frame.c:766	Heap-based Buffer Overflow	CVE-2025-11082
	libbfd.c:989	Out-of-bounds Write	CVE-2025-11413

in the call graph that can potentially reach the target as the guidance trace, rather than the LLM-predicted call stack. Figure 9 reports the speedup of STACZZER and these three configurations over the foundation fuzzer AFL. For SEEDPOOL and ENERGY, both yield clear speedups, but neither matches the improvement achieved by STACZZER when both are enabled, indicating that each modification contributes to the overall effectiveness. For CALLGRAPH, the speedup is only marginal, suggesting that call-graph-based trace guidance alone provides imprecise signals, and that refining it into a call stack via the LLM is key to the performance gains. **Overall, seed selection, power scheduling, and LLM-based call-stack prediction are all effective and necessary components.**

6.5 New Bugs

We use STACZZER to regression-test the latest project versions at patch locations for known fixed vulnerabilities from the controlled experiments in Table 2, with a 24-hour time limit. As shown in Table 7, we discover 10 new vulnerabilities in Binutils 2.45, located in objdump and the GNU linker ld. We reported all of them to the developers; they have been fixed and assigned CVE IDs. For these new vulnerabilities, we further perform incremental patch testing on the patched programs and identify two additional incomplete fixes, as shown in Table 8; the developers confirmed and fixed them. We list the CWE (Common Weakness Enumeration) for each vulnerability in both tables. These issues in widely deployed software can have severe impact: heap-based buffer overflows

and out-of-bounds writes enable illegal memory writes that can disrupt execution or even allow privilege escalation, while out-of-bounds reads can enable illegal memory access and information leakage. These findings demonstrate STACZZER’s practical value in real-world settings.

7 Threats to Validity

We discuss potential threats to validity in our experiments.

The main threat to internal validity is fuzzing randomness. Prior work [20] shows that at least 40 runs are needed to reduce DGF randomness to an acceptable level. We therefore run each fuzzer on each target 40 times, for a total cost of 58.4 CPU-years, which we believe largely mitigates randomness.

The main threats to external validity are that our approach ignores the order and frequency of executed call sites and does not handle vulnerabilities reachable through multiple call stacks, which can lead to suboptimal seed prioritization. Capturing full execution sequences or enumerating call stacks would significantly increase fuzzer overhead, so our design makes an explicit efficiency-precision trade-off. STACZZER is effective on the benchmark suite used by the SOTA DGF tool DAFL and also finds previously unknown vulnerabilities in real-world critical software that were later fixed, suggesting that its effectiveness generalizes to practical DGF settings.

8 Related Work

Our approach is related to (1) directed greybox fuzzing and (2) techniques that leverage LLMs to enhance fuzzing. We summarize the related work below.

Directed greybox fuzzing. AFLGo [5] pioneered DGF by prioritizing seeds using control-flow-graph distances to targets. Follow-up systems refine this idea from different angles, e.g., value-gap awareness (CAFL [21]), deviation blocks (WINDRANGER [11]), Monte Carlo guidance (MC² [36]), selective instrumentation (SELECTFUZZ [25]), value-flow guidance (DAFL [19]), dynamic indirect-call resolution (PDGF [44]), combined control/data-flow criticality (WAFLGo [39]), and learning-based mutation (IDFUZZ [9]). All these methods depend on imprecise static-analysis distance metrics. HAWKEYE [7] and SDFUZZ [22] incorporate target call stacks, but call stacks are hard to obtain and they still rely on imprecise distance metrics. Our experiments show STACZZER’s predicted call stack is a stronger metric. HALO [18] and DEEPGo [24] mitigate distance imprecision via invariant inference and reinforcement learning, respectively, but they are not open-source, preventing us from comparing with them. BEACON [16] prunes paths proven irrelevant by static analysis, complementing STACZZER’s seed prioritization. Multi-target DGF includes alarm-driven fuzzing [8, 32, 45, 46] and critical-set fuzzing [3, 17, 23, 34]; both rely on conventional distance metrics, and can incorporate STACZZER’s call-stack metric.

Fuzzing with LLMs. LLMs are widely used to generate initial corpora and mutators for structured-input fuzzing (e.g., compilers/interpreters/theorem provers) [12, 38, 41], non-textual inputs [43], deep-learning libraries [10], and protocols [27], and to synthesize harnesses [26]. They also assist directed fuzzing by producing vulnerability-triggering seeds [40, 47]. STACZZER is orthogonal and can be combined with these approaches. AD [4] uses LLMs to rescale static-analysis distances in DGF, but the metric remains imprecise due to inherent over-approximation; STACZZER instead uses predicted guidance traces to mitigate this issue.

9 Conclusion

To address the imprecision of static-analysis-based distance metrics in directed greybox fuzzing (DGF), we propose trace-guided directed greybox fuzzing (TDGF), which prioritizes seeds whose execution traces overlap more with a guidance trace. We study two guidance-trace types and find that coarse-grained call-stack traces provide guidance comparable to fine-grained control-flow

traces while being easier for large language models (LLMs) to predict. Based on this finding, we present STACZZER, which uses LLM-predicted vulnerability-triggering call stacks to guide seed prioritization in DGF. We evaluate STACZZER with experiments totaling 58.4 CPU-years: it reproduces known vulnerabilities with average speedups of $2.13\times$ to $3.14\times$ over baselines, and it discovers 10 new vulnerabilities and 2 incomplete fixes, with 10 assigned CVE IDs. These results show that STACZZER substantially improves directed vulnerability triggering over existing directed fuzzers.

References

- [1] Anthropic. 2025. Claude Code. <https://claude.com/product/claude-code>.
- [2] Anthropic. 2025. Claude-Opus-4.5. <https://www.anthropic.com/news/claude-opus-4-5>.
- [3] Andrew Bao, Wenjia Zhao, Yanhao Wang, Yueqiang Cheng, Stephen McCamant, and Pen-Chung Yew. 2025. From Alarms to Real Bugs: Multi-target Multi-step Directed Greybox Fuzzing for Static Analysis Result Verification. In *34th USENIX Security Symposium (USENIX Security 25)*. 6977–6997. <https://www.usenix.org/system/files/usenixsecurity25-bao-andrew.pdf>
- [4] Wang Bin, Ao Yang, Kedan Li, Aofan Liu, Hui Li, Guibo Luo, Weixiang Huang, and Yan Zhuang. 2025. Attention Distance: A Novel Metric for Directed Fuzzing with Large Language Models. arXiv:2512.19758 [cs.SE] <https://arxiv.org/abs/2512.19758>
- [5] Marcel Böhme, Van-Thuan Pham, Manh-Dung Nguyen, and Abhik Roychoudhury. 2017. Directed Greybox Fuzzing. In *Proceedings of the 2017 ACM SIGSAC Conference on Computer and Communications Security, CCS 2017, Dallas, TX, USA, October 30 - November 03, 2017*, Bhavani Thuraisingham, David Evans, Tal Malkin, and Dongyan Xu (Eds.). ACM, 2329–2344. doi:10.1145/3133956.3134020
- [6] Marcel Böhme, Van-Thuan Pham, and Abhik Roychoudhury. 2016. Coverage-based Greybox Fuzzing as Markov Chain. In *Proceedings of the 2016 ACM SIGSAC Conference on Computer and Communications Security, Vienna, Austria, October 24-28, 2016*, Edgar R. Weippl, Stefan Katzenbeisser, Christopher Kruegel, Andrew C. Myers, and Shai Halevi (Eds.). ACM, 1032–1043. doi:10.1145/2976749.2978428
- [7] Hongxu Chen, Yinxing Xue, Yuekang Li, Bihuan Chen, Xiaofei Xie, Xiuheng Wu, and Yang Liu. 2018. Hawkeye: Towards a Desired Directed Grey-box Fuzzer. In *Proceedings of the 2018 ACM SIGSAC Conference on Computer and Communications Security, CCS 2018, Toronto, ON, Canada, October 15-19, 2018*, David Lie, Mohammad Mannan, Michael Backes, and XiaoFeng Wang (Eds.). ACM, 2095–2108. doi:10.1145/3243734.3243849
- [8] Yaohui Chen, Peng Li, Jun Xu, Shengjian Guo, Rundong Zhou, Yulong Zhang, Tao Wei, and Long Lu. 2020. SAVIOR: Towards Bug-Driven Hybrid Testing. In *2020 IEEE Symposium on Security and Privacy, SP 2020, San Francisco, CA, USA, May 18-21, 2020*. IEEE, 1580–1596. doi:10.1109/SP40000.2020.00002
- [9] Yiyang Chen, Chao Zhang, Long Wang, Wenyu Zhu, Changhua Luo, Nuoqi Gui, Zheyu Ma, Xingjian Zhang, and Bingkai Su. 2025. {IDFuzz}: Intelligent Directed Grey-box Fuzzing. In *34th USENIX Security Symposium (USENIX Security 25)*. 6219–6238. <https://www.usenix.org/system/files/usenixsecurity25-chen-yiyang.pdf>
- [10] Yinlin Deng, Chunqiu Steven Xia, Haoran Peng, Chenyuan Yang, and Lingming Zhang. 2023. Large Language Models Are Zero-Shot Fuzzers: Fuzzing Deep-Learning Libraries via Large Language Models. In *Proceedings of the 32nd ACM SIGSOFT International Symposium on Software Testing and Analysis, ISSATA 2023, Seattle, WA, USA, July 17-21, 2023*, René Just and Gordon Fraser (Eds.). ACM, 423–435. doi:10.1145/3597926.3598067
- [11] Zhengjie Du, Yuekang Li, Yang Liu, and Bing Mao. 2022. Windranger: A Directed Greybox Fuzzer driven by Deviation Basic Blocks. In *44th IEEE/ACM 44th International Conference on Software Engineering, ICSE 2022, Pittsburgh, PA, USA, May 25-27, 2022*. ACM, 2440–2451. doi:10.1145/3510003.3510197
- [12] Jueon Eom, Seyeon Jeong, and Taekyoung Kwon. 2024. Fuzzing JavaScript Interpreters with Coverage-Guided Reinforcement Learning for LLM-Based Mutation. In *Proceedings of the 33rd ACM SIGSOFT International Symposium on Software Testing and Analysis, ISSATA 2024, Vienna, Austria, September 16-20, 2024*, Maria Christakis and Michael Pradel (Eds.). ACM, 1656–1668. doi:10.1145/3650212.3680389
- [13] Google. 2025. Gemini 2.5-pro. <https://docs.cloud.google.com/vertex-ai/generative-ai/docs/models/gemini/2-5-pro>.
- [14] Google. 2025. Gemini CLI. <https://geminicli.com>.
- [15] Myles Hollander, Douglas A Wolfe, and Eric Chickens. 2013. *Nonparametric statistical methods*. John Wiley & Sons.
- [16] Heqing Huang, Yiyuan Guo, Qingkai Shi, Peisen Yao, Rongxin Wu, and Charles Zhang. 2022. BEACON: Directed Grey-Box Fuzzing with Provable Path Pruning. In *43rd IEEE Symposium on Security and Privacy, SP 2022, San Francisco, CA, USA, May 22-26, 2022*. IEEE, 36–50. doi:10.1109/SP46214.2022.9833751
- [17] Heqing Huang, Peisen Yao, Hung-Chun Chiu, Yiyuan Guo, and Charles Zhang. 2024. Titan : Efficient Multi-target Directed Greybox Fuzzing. In *IEEE Symposium on Security and Privacy, SP 2024, San Francisco, CA, USA, May 19-23, 2024*. IEEE, 1849–1864. doi:10.1109/SP54263.2024.00059

- [18] Heqing Huang, Anshunkang Zhou, Mathias Payer, and Charles Zhang. 2024. Everything is Good for Something: Counterexample-Guided Directed Fuzzing via Likely Invariant Inference. In *IEEE Symposium on Security and Privacy, SP 2024, San Francisco, CA, USA, May 19-23, 2024*. IEEE, 1956–1973. doi:10.1109/SP54263.2024.00142
- [19] Tae Eun Kim, Jaeseung Choi, Kihong Heo, and Sang Kil Cha. 2023. DAFL: Directed Grey-box Fuzzing guided by Data Dependency. In *32nd USENIX Security Symposium, USENIX Security 2023, Anaheim, CA, USA, August 9-11, 2023*, Joseph A. Calandrino and Carmela Troncoso (Eds.). USENIX Association, 4931–4948. <https://www.usenix.org/conference/usenixsecurity23/presentation/kim-tae-eun>
- [20] Tae Eun Kim, Jaeseung Choi, Seongjae Im, Kihong Heo, and Sang Kil Cha. 2024. Evaluating Directed Fuzzers: Are We Heading in the Right Direction? *Proc. ACM Softw. Eng.* 1, FSE (2024), 316–337. doi:10.1145/3643741
- [21] Gwangmu Lee, Woochul Shim, and Byoungyoung Lee. 2021. Constraint-guided Directed Greybox Fuzzing. In *30th USENIX Security Symposium, USENIX Security 2021, August 11-13, 2021*, Michael D. Bailey and Rachel Greenstadt (Eds.). USENIX Association, 3559–3576. <https://www.usenix.org/conference/usenixsecurity21/presentation/lee-gwangmu>
- [22] Penghui Li, Wei Meng, and Chao Zhang. 2024. SDFuzz: Target States Driven Directed Fuzzing. In *33rd USENIX Security Symposium, USENIX Security 2024, Philadelphia, PA, USA, August 14-16, 2024*, Davide Balzarotti and Wenyuan Xu (Eds.). USENIX Association. <https://www.usenix.org/conference/usenixsecurity24/presentation/li-penghui>
- [23] Hongliang Liang, Xinglin Yu, Xianglin Cheng, Jie Liu, and Jin Li. 2024. Multiple Targets Directed Greybox Fuzzing. *IEEE Trans. Dependable Secur. Comput.* 21, 1 (2024), 325–339. doi:10.1109/TDSC.2023.3253120
- [24] Peihong Lin, Pengfei Wang, Xu Zhou, Wei Xie, Gen Zhang, and Kai Lu. 2024. DeepGo: Predictive Directed Greybox Fuzzing. In *31st Annual Network and Distributed System Security Symposium, NDSS 2024, San Diego, California, USA, February 26 - March 1, 2024*. The Internet Society. <https://www.ndss-symposium.org/ndss-paper/deepgo-predictive-directed-greybox-fuzzing/>
- [25] Changhua Luo, Wei Meng, and Penghui Li. 2023. SelectFuzz: Efficient Directed Fuzzing with Selective Path Exploration. In *44th IEEE Symposium on Security and Privacy, SP 2023, San Francisco, CA, USA, May 21-25, 2023*. IEEE, 2693–2707. doi:10.1109/SP46215.2023.10179296
- [26] Yunlong Lyu, Yuxuan Xie, Peng Chen, and Hao Chen. 2024. Prompt Fuzzing for Fuzz Driver Generation. In *Proceedings of the 2024 on ACM SIGSAC Conference on Computer and Communications Security, CCS 2024, Salt Lake City, UT, USA, October 14-18, 2024*, Bo Luo, Xiaojing Liao, Jun Xu, Engin Kirda, and David Lie (Eds.). ACM, 3793–3807. doi:10.1145/3658644.3670396
- [27] Ruijie Meng, Martin Mirchev, Marcel Böhme, and Abhik Roychoudhury. 2024. Large Language Model guided Protocol Fuzzing. In *31st Annual Network and Distributed System Security Symposium, NDSS 2024, San Diego, California, USA, February 26 - March 1, 2024*. The Internet Society. <https://www.ndss-symposium.org/ndss-paper/large-language-model-guided-protocol-fuzzing/>
- [28] MITRE. 2016. CVE-2016-4489. <https://cve.mitre.org/cgi-bin/cvename.cgi?name=CVE-2016-4489>.
- [29] OpenAI. 2025. Codex. <https://openai.com/codex/>.
- [30] OpenAI. 2025. GPT-5.1. <https://openai.com/index/gpt-5-1/>.
- [31] OpenAI. 2025. GPT-5.1-Codex-Max. <https://openai.com/index/gpt-5-1-codex-max/>.
- [32] Sebastian Österlund, Kaveh Razavi, Herbert Bos, and Cristiano Giuffrida. 2020. ParmeSan: Sanitizer-guided Greybox Fuzzing. In *29th USENIX Security Symposium, USENIX Security 2020, August 12-14, 2020*, Srdjan Capkun and Franziska Roesner (Eds.). USENIX Association, 2289–2306. <https://www.usenix.org/conference/usenixsecurity20/presentation/osterlund>
- [33] Henry Gordon Rice. 1953. Classes of recursively enumerable sets and their decision problems. *Transactions of the American Mathematical society* 74, 2 (1953), 358–366.
- [34] Huanyao Rong, Wei You, Xiaofeng Wang, and Tianhao Mao. 2024. Toward Unbiased Multiple-Target Fuzzing with Path Diversity. In *33rd USENIX Security Symposium, USENIX Security 2024, Philadelphia, PA, USA, August 14-16, 2024*, Davide Balzarotti and Wenyuan Xu (Eds.). USENIX Association. <https://www.usenix.org/conference/usenixsecurity24/presentation/rong>
- [35] Konstantin Serebryany, Derek Bruening, Alexander Potapenko, and Dmitriy Vyukov. 2012. AddressSanitizer: A Fast Address Sanity Checker. In *Proceedings of the 2012 USENIX Annual Technical Conference, USENIX ATC 2012, Boston, MA, USA, June 13-15, 2012*, Gernot Heiser and Wilson C. Hsieh (Eds.). USENIX Association, 309–318. <https://www.usenix.org/conference/atc12/technical-sessions/presentation/serebryany>
- [36] Abhishek Shah, Dongdong She, Samanway Sadhu, Krish Singal, Peter Coffman, and Suman Jana. 2022. MC2: Rigorous and Efficient Directed Greybox Fuzzing. In *Proceedings of the 2022 ACM SIGSAC Conference on Computer and Communications Security, CCS 2022, Los Angeles, CA, USA, November 7-11, 2022*, Heng Yin, Angelos Stavrou, Cas Cremers, and Elaine Shi (Eds.). ACM, 2595–2609. doi:10.1145/3548606.3560648
- [37] Yulei Sui and Jingling Xue. 2016. SVF: interprocedural static value-flow analysis in LLVM. In *Proceedings of the 25th International Conference on Compiler Construction, CC 2016, Barcelona, Spain, March 12-18, 2016*, Ayal Zaks and Manuel V. Hermenegildo (Eds.). ACM, 265–266. doi:10.1145/2892208.2892235

- [38] Chunqiu Steven Xia, Matteo Paltenghi, Jia Le Tian, Michael Pradel, and Lingming Zhang. 2024. Fuzz4All: Universal Fuzzing with Large Language Models. In *Proceedings of the 46th IEEE/ACM International Conference on Software Engineering, ICSE 2024, Lisbon, Portugal, April 14-20, 2024*. ACM, 126:1–126:13. doi:10.1145/3597503.3639121
- [39] Yi Xiang, Xuhong Zhang, Peiyu Liu, Shouling Ji, Xiao Xiao, Hong Liang, Jiacheng Xu, and Wenhai Wang. 2024. Critical Code Guided Directed Greybox Fuzzing for Commits. In *33rd USENIX Security Symposium, USENIX Security 2024, Philadelphia, PA, USA, August 14-16, 2024*, Davide Balzarotti and Wenyuan Xu (Eds.). USENIX Association. <https://www.usenix.org/conference/usenixsecurity24/presentation/xiang-yi>
- [40] Yi-Jiang Xu, Hong-Rui Jia, Li-Guo Chen, Xin Wang, Zheng-Ran Zeng, Yi-Dong Wang, Qing Gao, Wei Ye, Shi-Kun Zhang, and Zhong-Hai Wu. 2025. ISC4DGF: Enhancing Directed Grey-Box Fuzzing with Initial Seed Corpus Generation Driven by Large Language Models. *Journal of Computer Science and Technology* 40, 6 (2025), 1662–1677. doi:10.1007/s11390-025-4745-0
- [41] Yupeng Yang, Shenglong Yao, Jizhou Chen, and Wenke Lee. 2025. Hybrid Language Processor Fuzzing via {LLM-Based} Constraint Solving. In *34th USENIX Security Symposium (USENIX Security 25)*. 6299–6318. <https://www.usenix.org/system/files/usenixsecurity25-yang-yupeng.pdf>
- [42] Michał Zalewski. 2013. American Fuzzy Lop. <https://lcamtuf.coredump.cx/afl/>.
- [43] Kunpeng Zhang, Zongjie Li, Daoyuan Wu, Shuai Wang, and Xin Xia. 2025. Low-Cost and Comprehensive Non-textual Input Fuzzing with LLM-Synthesized Input Generators. *arXiv preprint arXiv:2501.19282* (2025). <https://www.usenix.org/system/files/conference/usenixsecurity25/sec25cycle1-prepub-1291-zhang-kunpeng.pdf>
- [44] Yujian Zhang, Yaokun Liu, Jinyu Xu, and Yanhao Wang. 2024. Predecessor-aware Directed Greybox Fuzzing. In *IEEE Symposium on Security and Privacy, SP 2024, San Francisco, CA, USA, May 19-23, 2024*. IEEE, 1884–1900. doi:10.1109/SP54263.2024.00040
- [45] Zhijie Zhang, Liwei Chen, Haolai Wei, Gang Shi, and Dan Meng. 2024. Prospector: Boosting Directed Greybox Fuzzing for Large-Scale Target Sets with Iterative Prioritization. In *Proceedings of the 33rd ACM SIGSOFT International Symposium on Software Testing and Analysis, ISSTA 2024, Vienna, Austria, September 16-20, 2024*, Maria Christakis and Michael Pradel (Eds.). ACM, 1351–1363. doi:10.1145/3650212.3680365
- [46] Han Zheng, Jiayuan Zhang, Yuhang Huang, Zezhong Ren, He Wang, Chunjie Cao, Yuqing Zhang, Flavio Toffalini, and Mathias Payer. 2023. FISHFUZZ: Catch Deeper Bugs by Throwing Larger Nets. In *32nd USENIX Security Symposium, USENIX Security 2023, Anaheim, CA, USA, August 9-11, 2023*, Joseph A. Calandrino and Carmela Troncoso (Eds.). USENIX Association, 1343–1360. <https://www.usenix.org/conference/usenixsecurity23/presentation/zheng>
- [47] Zhuotong Zhou, Yongzhuo Yang, Susheng Wu, Yiheng Huang, Bihuan Chen, and Xin Peng. 2024. Magneto: A Step-Wise Approach to Exploit Vulnerabilities in Dependent Libraries via LLM-Empowered Directed Fuzzing. In *Proceedings of the 39th IEEE/ACM International Conference on Automated Software Engineering, ASE 2024, Sacramento, CA, USA, October 27 - November 1, 2024*, Vladimir Filkov, Baishakhi Ray, and Minghui Zhou (Eds.). ACM, 1633–1644. doi:10.1145/3691620.3695531